



ELSEVIER

# Investigation of the aluminium-ruthenium phase diagram above 25 at.% ruthenium

T.D. Boniface, L.A. Cornish\*

*The University of the Witwatersrand, Johannesburg, South Africa*

Received 25 January 1995; in final form 6 June 1995

## Abstract

Alloys of ruthenium content above nominally 25 at.% were manufactured, investigated using optical and scanning electron microscopy, and analysed by EDS, electron spectroscopy, X-ray diffraction and thermal analysis. The results indicated that there is a peritectic cascade involving the phases  $Al_3Ru_2$ ,  $Al_2Ru$  and  $Al_{13}Ru_4$ . Previous work had indicated that the last phase in the cascade was  $Al_6Ru$ , with a eutectic reaction between  $Al_6Ru$  and  $Al(Ru)$ . The occasional absence of  $Al_2Ru$  is explained by the closeness of its formation temperature to that of  $Al_{13}Ru_4$ , such that undercooling can miss the reaction. The phase diagram reactions, formation temperatures and phase widths were modified accordingly.

**Keywords:** Al-Ru phase diagram; Al-poor end

## 1. Introduction

Work was undertaken on the aluminium-ruthenium system after Fleischer [1] identified the potential of the  $AlRu$  phase for high temperature applications. Modifications to the binary phase diagram are suggested after published data were found to disagree [2], and experimental investigations revealed differing formation reactions and phase widths, compared with those previously published.

Obrowski [3] reported  $AlRu$  to form congruently, then react peritectically to form  $Al_3Ru_2$ , with the latter being involved in a eutectic reaction with  $Al_6Ru$  (which also formed congruently). The phases  $Al_3Ru$  and  $Al_2Ru$  formed in the solid state at lower temperatures. There was another eutectic between  $AlRu$  and  $Ru(Al)$ . Anlage et al. [4] investigated the phase diagram up to 20 at.% Ru, and reported the phases  $Al(Ru)$ ,  $Al_6Ru$  and  $Al_{13}Ru_4$  (Obrowski's  $Al_3Ru$ ). Using thermal analysis, the eutectic reaction  $L \rightarrow Al_6Ru + Al(Ru)$  was found to be at 652°C, the peritectic reaction  $L + Al_{13}Ru_4 \rightarrow Al_6Ru$  occurred at 723°C, and the peritectic formation of  $Al_{13}Ru_4$  was at 1403°C.

X-ray studies were undertaken by a number of

workers. Schwomma et al. [5] identified  $Al_2Ru$  and  $AlRu$  in samples comprising 33.3 at.% Ru. Edshammar [6-8] investigated  $Al_{13}Ru_4$ ,  $AlRu$ ,  $Al_3Ru_2$ ,  $Al_2Ru$ , and a phase observed only in arc-melted samples,  $Al_{\sim 2.5}Ru$ .  $Al_3Ru_2$  formed in samples with 36.36-44.44 at.% Ru after heat treating at 950°C.  $Al_2Ru$  formed after heat treating alloys with 27-30.77 at.% Ru, and was also present in some as-cast alloys. Edshammar also reported additional CsCl-like phases, i.e.  $AlRu$  variations, but gave one structure [7]. Later investigation [8] reported  $Al_6Ru$ , but not  $Al_{12}Ru$ , despite annealing below Obrowski's specified temperature of formation. Varich and Lyukevich [9] used rapid solidification techniques to find the maximum solubility of ruthenium in  $Al(Ru)$ , 3.23 at.% Ru.

## 2. Experimental

Samples were manufactured from elemental powders or chunks (of not less than 99% purity) by arc-melting under argon, as discussed in detail previously [10,11]. Alternatively, a zirconia crucible in an induction furnace with an argon atmosphere was used. Heat treatments were undertaken in sealed silica ampoules, under vacuum.

Optical microscopy was undertaken after etching

\* Corresponding author.

with Murakami's reagent (10 g  $K_3Fe(CN)_6$ , 10 g KOH, and 100 ml  $H_2O$ ) for up to 30 s. Electron microscopy was done with Hitachi S-450 and JEOL JSM-840A scanning electron microscopes (SEMs). Electron microscopy (JEOL Superprobe) results from the  $Al_{68}:Ru_{32}$  sample (deemed the most homogeneous) were used to calibrate the Hitachi SEM, to enable quantitative EDS analysis with standards.

Debye-Scherrer powder diffraction was carried out as described previously [10,11]. A Philips PW X-ray generator was used, with a copper anode and nickel filter. The film exposure time was 24 h, and the films were compared against published data from JCPDS-CD ROM [12], and calculated data for  $Al_3Ru$ . The latter data was computed from the 'CC Miller' program (Shareware package by C.L. Churms, Somerset West, RSA), by inputting atom positions for the  $Ni_3Ti$  structure type [13].

Thermal analysis was conducted with a TA Instruments SDT 2960 TGA/DTA on the nominal  $Al_{72}:Ru_{28}$  sample. The sample was heated three times up to 1480°C, in a nitrogen atmosphere (flowrate 100  $mm^3\ min^{-1}$ ), and the third heating cycle did not have an inert atmosphere. A Netzsch STA 409EP TGA/DTA was also used, with an argon atmosphere (and same flowrate). Alumina crucibles were used, and the specimens ( $Al_{72}:Ru_{28}$  and  $Al_{63}:Ru_{37}$ ) were in powder form. Only the third data run was used.

### 3. Results and discussion

There is a tendency for the alloys in this investigation to be inhomogeneous. This is due to many factors, mainly the large difference in the melting points of aluminium and ruthenium (660°C and 2334°C respectively), the existence of a high temperature intermetallic phase ( $AlRu$ ), and the presence of a number of adjacent peritectic reactions, resulting in a very steep liquidus between 50% ( $AlRu$ ) and near 0% Ru. The situation was exacerbated because high temperatures were needed to melt ruthenium, and this allowed the formation of higher temperature and higher ruthenium-content phases, which might not have formed if lower temperatures could have been employed. Samples were arc-melted to achieve the high temperatures, but this unfortunately resulted in fast cooling, and the peritectic reactions could not go to completion. Thus many compounds, at least partially, formed directly from the melt, and these were highly cored. The differing densities were also a source of inhomogeneity (ruthenium is considerably denser than aluminium), since the higher ruthenium-content compounds tended to sink, depleting the melt of ruthenium, thus encouraging the formation of less Ru-rich phases. An additional problem was aluminium

loss due to its high vapour pressure. There were also sampling errors for X-ray samples, since small amounts of powder were removed from relatively large and inhomogeneous samples.

The phase widths were derived using the most reproducible analyses from the more homogeneous alloys, and are shown with earlier results [10,11] in Table 1. Debye-Scherrer analyses were undertaken to confirm the phases, but high angle lines could not be measured for accurate lattice parameter measurements. Very faint lines were identified as belonging to  $Al_2O_3$  phases, but as the EDS weight percentage totals were correct, the oxides were assumed to have formed on the surface during powder preparation. Comparison of the *d*-spacings of phases in different samples agreed to within about 0.001 nm, but there was no indication that phases with wider stability ranges showed greater variation in *d*-spacing, as might be expected. The *d*-spacings were found to agree well with published data.

The as-cast nominal  $Al_{72}:Ru_{28}$  sample comprised mainly discrete  $Al_2Ru$  particles, with adjacent small amounts of  $Al_3Ru_2$ , in an  $Al_{13}Ru_4$  matrix (Fig. 1). Debye-Scherrer data confirmed the presence of

Table 1  
Phase composition ranges

Phase	Al-rich boundary (at.% Ru)	Ru-rich boundary (at.% Ru)
$Al_6Ru$	$15.10 \pm 1$	$15.7 \pm 1$
$Al_{13}Ru_4$	$25.00 \pm 1.5$	$26.6 \pm 1.5$
$Al_2Ru$	$30.35 \pm 1$	$35.8 \pm 1$
$Al_3Ru_2$	$35.7 \pm 1$	$41.6 \pm 1$
$AlRu$	$42 \pm 3$	$54.3 \pm 1$

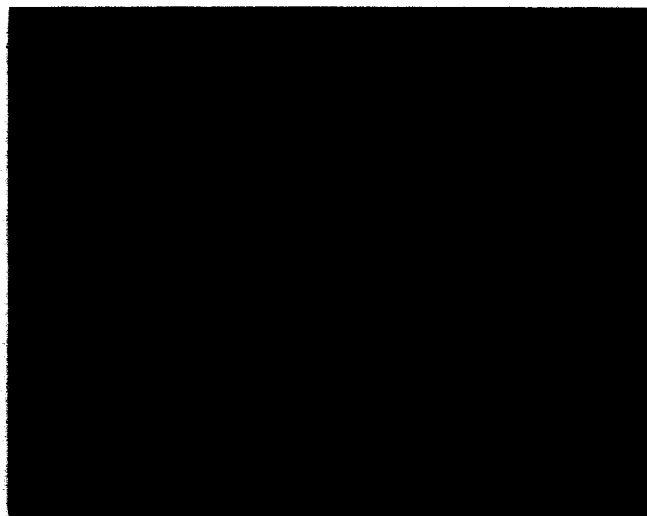


Fig. 1. SEM micrograph (secondary electron mode) of nominal  $Al_{72}:Ru_{28}$  before heat treatment.  $Al_3Ru_2$  (white),  $Al_2Ru$  (light grey grains),  $Al_{13}Ru_4$  (dark grey matrix).

$\text{Al}_{13}\text{Ru}_4$  with small amounts of  $\text{Al}_3\text{Ru}_2$ . The former was deduced to be  $\text{Al}_{13}\text{Ru}_4$ , rather than  $\text{Al}_3\text{Ru}$ , because there were two 100% intensity peaks instead of one. It is likely that  $\text{Al}_2\text{Ru}$  was missed because of sampling error.

After heat treatment a different structure was revealed, because the sample was still inhomogeneous and a different cross section was sampled. The phases formed layers around a core of  $\text{AlRu}$  (with an interdendritic eutectic of  $\text{AlRu} + \text{Ru(Al)}$ ). The layers working outwards from the core were:  $\text{Al}_3\text{Ru}_2$ ,  $\text{Al}_2\text{Ru}$ , and finally  $\text{Al}_{13}\text{Ru}_4$  with discrete  $\text{Al}_6\text{Ru}$ . The  $\text{Al}_2\text{Ru}$  layer was very cracked and porous (Fig. 2). X-ray diffraction confirmed  $\text{Al}_2\text{Ru}$  and  $\text{Al}_{13}\text{Ru}_4$ , with traces of  $\text{Al}_3\text{Ru}_2$ .

The first thermal analysis scan had endothermic reactions with onset temperatures 656°C (peaking at 660°C), and 730°C (peaking at 741°C), and an exothermic reaction with an onset temperature of 795°C (peaking at 803°C). These reactions are the  $\text{Al}(\text{Ru}) + \text{Al}_6\text{Ru}$  eutectic and melting point of aluminium for the first peak, and formation of  $\text{Al}_6\text{Ru}$  (Anlage et al. [4]) for the second. Peaks for the second and third runs were endothermic. The onset values for the third were 1343°C (peaking at 1355°C) and 1416°C (peaking at 1428°C). The lower peak was much smaller, and is not yet identified, but could be due to an oxide reaction since it was greater on the third scan, which was not run under a protective atmosphere. However, Obrowski reported a reaction at about 1300°C [3]. The upper peak is fairly close to that described by Anlage et al. [4] of 1403°C for the formation of  $\text{Al}_{13}\text{Ru}_4$ . There was also a slight endothermic peak at about 1460°C which might be due to the formation of  $\text{Al}_2\text{Ru}$ .

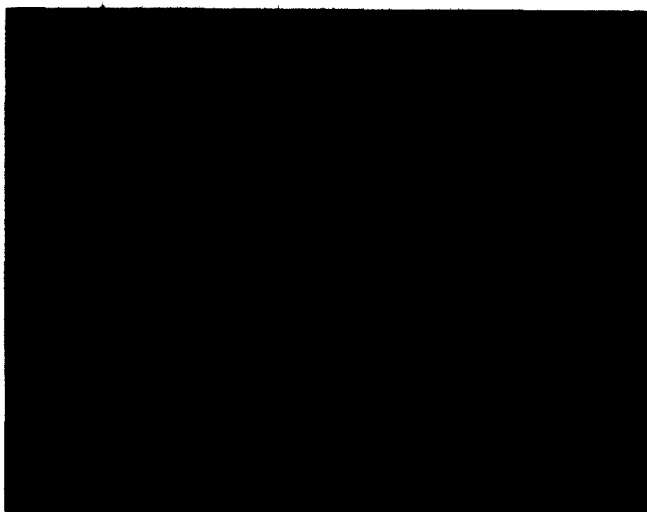


Fig. 2. SEM micrograph (secondary electron mode) of nominal  $\text{Al}_{72}\text{:Ru}_{28}$  annealed at 1300°C for 6.5 h, showing some of the layers. Working upwards from the bottom of the micrograph: core layer  $\text{AlRu}$  (light grey) with interdendritic regions of  $\text{Ru(Al)}$  (white),  $\text{Al}_3\text{Ru}_2$  (dark grey layer with porosity), and  $\text{Al}_2\text{Ru}$  (black).

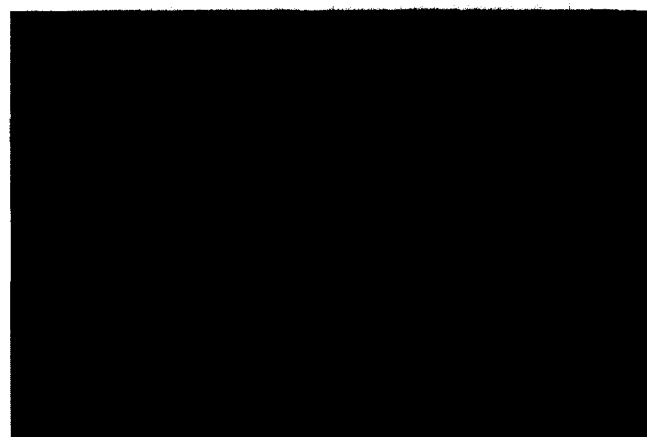


Fig. 3. Optical micrograph of nominal  $\text{Al}_{68}\text{:Ru}_{32}$  annealed at 1200°C for 312 h (etched with Murakami's reagent).  $\text{Al}_2\text{Ru}$  (white dendrites),  $\text{Al}_{13}\text{Ru}_4$  (dark grey), cracks and pores (black).

The nominal  $\text{Al}_{68}\text{:Ru}_{32}$  sample comprised irregular dendrites of  $\text{Al}_2\text{Ru}$  surrounded by a matrix of  $\text{Al}_{13}\text{Ru}_4$  (Fig. 3), indicating that  $\text{Al}_2\text{Ru}$  has a higher melting point than  $\text{Al}_{13}\text{Ru}_4$ , and the probable peritectic formation of  $\text{Al}_{13}\text{Ru}_4$ . X-ray data confirmed the  $\text{Al}_2\text{Ru}$  and  $\text{Al}_{13}\text{Ru}_4$  phases.

The sample of nominal composition  $\text{Al}_{65}\text{:Ru}_{35}$  was produced in an induction furnace, and at about 950°C an exothermic reaction occurred. The microstructure was mainly irregular  $\text{Al}_2\text{Ru}$  dendrites in an  $\text{Al}_{13}\text{Ru}_4$  matrix. There was also a small region of  $\text{AlRu}$  enclosed in an  $\text{Al}_2\text{Ru}$  dendrite (Fig. 4). The irregular outline of both  $\text{Al}_2\text{Ru}$  and  $\text{AlRu}$  again suggest peritectic reactions. The small, uneven particles between the dendrite arms were not identified as eutectic in nature since their morphology was too irregular. They are

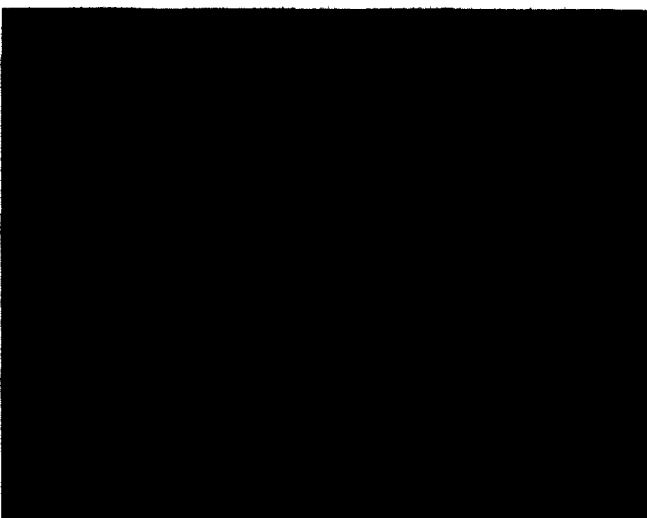


Fig. 4. SEM micrograph (back-scattered electron mode) of nominal  $\text{Al}_{65}\text{:Ru}_{35}$ .  $\text{AlRu}$  (small light region),  $\text{Al}_2\text{Ru}$  (darker grey),  $\text{Al}_{13}\text{Ru}_4$  (darkest grey).



Fig. 5. SEM micrograph (secondary electron mode) of nominal  $\text{Al}_{63}:\text{Ru}_{35}$ . Light grey dendrites of  $\text{Al}_2\text{Ru}$  (D), with irregular interdendritic regions comprising  $\text{Al}_2\text{Ru}$  (light grey) and  $\text{Al}_{13}\text{Ru}_4$  (dark grey). Note the rounded patches of  $\text{Al}_{13}\text{Ru}_4$  with  $\text{Al}_2\text{Ru}$  precipitated within.

thought to originate from decomposition of local inhomogeneities. Near-circular two-phase patches were observed between the dendrite arms (Fig. 5). The roundness of these areas suggests that  $\text{Al}_{13}\text{Ru}_4$  formed from the melt, and then fine  $\text{Al}_2\text{Ru}$  particles precipitated. This suggests that the formation temperatures of  $\text{Al}_2\text{Ru}$  and  $\text{Al}_{13}\text{Ru}_4$  are close. Debye-Scherrer data confirmed that the major phases were  $\text{Al}_2\text{Ru}$  and  $\text{Al}_{13}\text{Ru}_4$ .

The nominal  $\text{Al}_{63}:\text{Ru}_{37}$  sample exhibited a core of  $\text{AlRu}$  surrounded by successive layers of  $\text{Al}_3\text{Ru}_2$  and  $\text{Al}_{13}\text{Ru}_4$  (Fig. 6). The interface between  $\text{AlRu}$  and  $\text{Al}_3\text{Ru}_2$  is irregular, and suggests a peritectic reaction, whereas that between  $\text{Al}_3\text{Ru}_2$  and  $\text{Al}_{13}\text{Ru}_4$  is



Fig. 6. Optical micrograph of nominal  $\text{Al}_{63}:\text{Ru}_{37}$  annealed at 1200°C for 168 h (Murakami's etch).  $\text{Ru}(\text{Al})$  (white),  $\text{AlRu}$  (uncracked, light matrix),  $\text{Al}_3\text{Ru}_2$  (thin layer),  $\text{Al}_2\text{Ru}$  (cracked, dark matrix) containing  $\text{Al}_3\text{Ru}_2$  grains.



Fig. 7. SEM micrograph (back-scattered electron mode) of nominal  $\text{Al}_{63}:\text{Ru}_{37}$  annealed at 1200°C for 168 h. Uncracked region:  $\text{AlRu}$  (light grey),  $\text{Al}_3\text{Ru}_2$  (dark grey).

smoother, which could be due to  $\text{Al}_2\text{Ru}$  being formed and subsequently consumed. The precipitation of  $\text{Al}_3\text{Ru}_2$  on  $\text{AlRu}$  grain boundaries (Fig. 7), suggests a solid state transformation. The area analysis was approximately 42 at.% Ru, which supports Obrowski's phase diagram [3]. Debye-Scherrer data showed the presence of  $\text{AlRu}$ ,  $\text{Al}_3\text{Ru}_2$  and  $\text{Al}_2\text{Ru}$ .

During arc-melting of nominal  $\text{Al}_{53}:\text{Ru}_{47}$ , a slow exothermic reaction was observed. The microstructure was very similar to that of an  $\text{Al}_{50}:\text{Ru}_{50}$  sample; the centre was nearly single phase  $\text{AlRu}$ , with more  $\text{AlRu} + \text{Ru}(\text{Al})$  eutectic regions near the edges. Image analysis showed that approximately 4 at.% loss of aluminium had occurred from the outer regions. The phases were confirmed by Debye-Scherrer analysis.

Previous studies [10,11,14] showed that there was a cascade of peritectic reactions from (congruently formed)  $\text{AlRu}$  through the phases:  $\text{Al}_3\text{Ru}_2$ ,  $\text{Al}_2\text{Ru}$ ,  $\text{Al}_{13}\text{Ru}_4$ , and  $\text{Al}_6\text{Ru}$ . The presence of the  $\text{Al}_2\text{Ru}$  phase in as-cast samples indicates its stability at higher temperatures than reported by Obrowski [3]. The peritectic cascade is suggested by many samples showing layers with uneven dendrite edges. The sequence of the layered phases varies; occasionally  $\text{Al}_3\text{Ru}_2$  (Fig. 4) or  $\text{Al}_2\text{Ru}$  (Fig. 8) is absent. These phases could have formed in small amounts and then been consumed in a subsequent peritectic reaction, or had their formation suppressed by undercooling. The latter might be encouraged by the nearness of the formation temperatures in the peritectic cascade. The closeness of the temperatures of formation of  $\text{Al}_2\text{Ru}$  and  $\text{Al}_{13}\text{Ru}_4$  was suggested by the near-circular patches of  $\text{Al}_{13}\text{Ru}_4$  (Fig. 5). The slight endothermic peak at about 1460°C for the  $\text{Al}_{72}:\text{Ru}_{28}$  specimen is suggested to be the formation temperature of  $\text{Al}_2\text{Ru}$ .



Fig. 8. SEM micrograph (secondary electron mode) of nominal  $\text{Al}_{90}\text{:Ru}_{10}$  annealed at 475°C for 168 h.  $\text{AlRu}$  (light grey),  $\text{Al}_3\text{Ru}_2$  (first layer),  $\text{Al}_{13}\text{Ru}_4$  (second layer),  $\text{Al}_6\text{Ru}$  (third layer),  $\text{Al}(\text{Ru})$  (black matrix).

Thermal analysis was not conducted at high enough temperatures to locate the  $\text{Al}_3\text{Ru}_2$  formation temperature, but did show that the phase was stable to about 976°C, which is similar to Edshammar's heat treatment temperature [7].

The cascade of peritectic reactions, reaction temperatures, new phase composition ranges, and data from the peritectic reaction estimation [15] were

compiled to modify the phase diagram (Fig. 9). The lines are shown as dotted because there is still some uncertainty. The low ruthenium end used data from Anlage et al. [4], since there was good agreement. The major differences from Obrowski's diagram [3] are: the peritectic cascade, the peritectic (rather than solid state) formation of  $\text{Al}_2\text{Ru}$ , the absence of the  $\text{Al}_6\text{Ru} + \text{Al}_3\text{Ru}_2$  eutectic, the peritectic (rather than congruent) formation of  $\text{Al}_6\text{Ru}$ , and the absence of  $\text{Al}_{12}\text{Ru}$ .

### Acknowledgements

The sponsorship of Mintek, Randburg, RSA, is gratefully acknowledged. In addition, the authors thank M.B. Cortie, I.M. Wolff, I. Klingbiel and A. Wedepohl for their special help, and the Electron Microscope Unit, at the University of the Witwatersrand, for use of the facilities.

### References

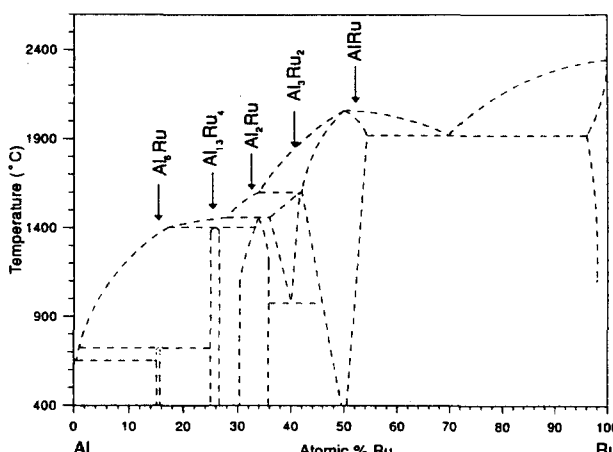


Fig. 9. Modified Al–Ru phase diagram.

- [1] R.L. Fleischer, *J. Mater. Sci.*, 22 (1987) 2281.
- [2] T.D. Boniface and L.A. Cornish, submitted to *J. Alloys Comp.*
- [3] W. Obrowski, *Metallwissenschaft und Technik (Berlin)*, 17 (1963) 108.
- [4] S.M. Anlage, P. Nash, R. Ramachandran and R.B. Schwarz, *J. Less-Common Met.*, 136 (1988) 237.
- [5] O. Schwomma, H. Nowotny and A. Wittmann, *Monatshefte für Chemie*, 94 (1963) 924.
- [6] L. Edshammar, *Acta Chem. Scand.*, 19 (1965) 2124.
- [7] L. Edshammar, *Acta Chem. Scand.*, 20 (1966) 427.
- [8] L. Edshammar, *Acta Chem. Scand.*, 22 (1968) 2374.
- [9] A.N. Varich and R.B. Lyukovich, *Russ. Metall.*, 1 (1973) 73.
- [10] T.D. Boniface, *The ruthenium–aluminium phase diagram*, M.Sc. Dissertation, The University of the Witwatersrand, Johannesburg, 1994.
- [11] T.D. Boniface and L.A. Cornish, submitted to *J. Alloys Comp.*
- [12] Joint Committee on Powder Diffraction Standards, International Centre for Diffraction Data, PA, USA, 1989.
- [13] P. Villars and L.D. Calvert, *Pearson's Handbook of Crystallographic Data for Intermetallic Phases*, Vol. 2. American Society for Metals, 1985.
- [14] T.D. Boniface and L.A. Cornish, *Proc. Electron Microsc. Soc. South Afr.*, 23 (1993) 61.
- [15] T.D. Boniface and L.A. Cornish, *Sino–South African Symp. on Materials Testing, Tainan, Taiwan, December 1994*, p. 173.